

SUPPLEMENTARY MATERIALS

Diffuse scattering intensity near the Bragg reflection in a (para)magnetic bulk f.c.c. Ni₃Fe-type permalloy

Sergiy M. Bokoch,^a Valentyn A. Tatarenko,^b and Iryna V. Vernyhora^{b,c}

^a*Institute for Advanced Materials Science and Innovative Technologies,*

Department of Materials Design and Technology, 15 Saulėtekio Ave., LT-10224 Vilnius, Lithuania

^b*G. V. Kurdyumov Institute for Metal Physics, N.A.S. of Ukraine,*

Department of Solid State Theory, 36 Academician Vernadsky Blvd., UA-03680 Kyiv-142, Ukraine

^c*Institute for Applied Physics, N.A.S. of Ukraine, Department of Modeling of Radiation Effects and Microstructure Transformations in Construction Materials, 58 Petropavlivska Str., UA-40030 Sumy, Ukraine*

1. Magnetic ‘mixing’ energy in f.c.c. Ni–Fe alloys

The expression connecting the Curie temperature of a magnetic phase transition with ‘pairwise’ ‘exchange’-interaction parameters, composition, and atomic long-range order (LRO) parameters for f.c.c. Ni–Fe-type alloy in a macroscopically homogeneous state [1–4] is as follows:

$$\begin{aligned} T_C \approx & -\frac{1}{6k_B} \left[1 + s_{Ni} s_{Ni} \tilde{J}_{NiNi} \mathbf{0} \right] \mathbf{1} - c \Theta + \left[1 + s_{Fe} s_{Fe} \tilde{J}_{FeFe} \mathbf{0} \right] c \Xi - \\ & - \left[\left(1 + s_{Ni} s_{Ni} \tilde{J}_{NiNi} \mathbf{0} \right) \mathbf{1} - c \Theta - \left(1 + s_{Fe} s_{Fe} \tilde{J}_{FeFe} \mathbf{0} \right) c \Xi \right]^2 + \\ & + 4 \left(1 + s_{Ni} s_{Ni} \right) \left(1 + s_{Fe} s_{Fe} \tilde{J}_{NiFe}^2 \mathbf{0} \right) \mathbf{1} - c c \Psi^2^{1/2}, \end{aligned} \quad (1.1)$$

where coefficients, Θ , Ξ and Ψ , are defined as follow:

$$\Theta = 1 - \frac{1}{16} \frac{\eta_c^2}{(1-c)^2}, \quad \Xi = 1 - \frac{1}{16} \frac{\eta_c^2}{c^2}, \quad \Psi = 1 + \frac{1}{16} \frac{\eta_c^2}{c(1-c)}, \quad (1.2)$$

where $\eta_c = \eta_c(c)$ is the equilibrium atomic-LRO parameter at the Curie point, $T_C = T_C(c)$. Equation (1.1) is valid for a $L1_2$ -type atomic-LRO state. In case of the $L1_0$ -type LRO state, it is necessary to replace the factor 1/16 in (1.2) by 1/12. For the atomic-SRO (disordered) solid solutions, where $\eta_c \equiv 0$, equation (1.1) becomes simpler. In this case for f.c.c.-Ni–Fe alloys, it is possible to determine values of Fourier components of ‘exchange’ ‘integrals’, $\tilde{J}_{NiNi} \mathbf{0}$, $\tilde{J}_{FeFe} \mathbf{0}$ and $\tilde{J}_{NiFe} \mathbf{0}$, at the fixed values of spin numbers, s_{Ni} and s_{Fe} , with use of experimental data on the concentration-dependent Curie temperature for these alloys. Experimental data and fitting curve, obtained according to (1.1), are shown in Fig. S1.1. The Fourier components of ‘exchange’ ‘integrals’ estimated by the fitting of (1.1) to experimental data on Curie temperatures [5, 6] (Fig. S1.1) are listed in Table S1.1. (These energy parameters have been calculated for several possible combinations of total spin numbers values, s_{Ni} and s_{Fe} , for Ni and Fe atoms, respectively.)

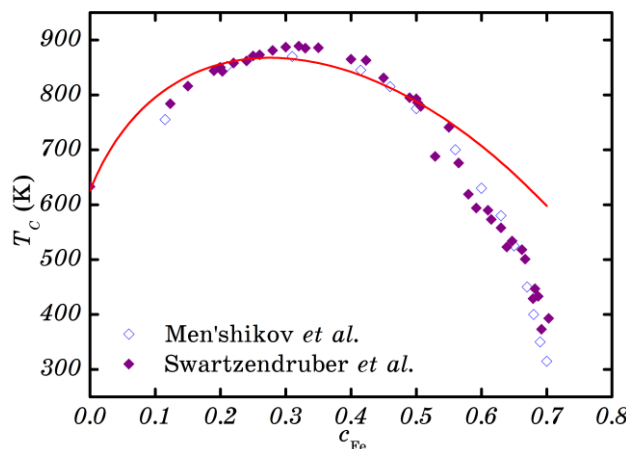


Figure S1.1 Concentration dependence of Curie temperature for f.c.c. Ni–Fe alloys, $T_C(c_{Fe})$, corresponding to the experimental data (\blacklozenge , \diamond) [5, 6], and the fitting curve (red solid line) plotted according to (1.1).

TABLE S1.1. Fourier components of ‘exchange’ ‘integrals’ for magnetic interactions, $\{\tilde{J}_{\beta\beta'} \mathbf{k}\}$, evaluated for f.c.c. Ni–Fe alloys (in accordance with [2, 4]).

s_{Ni}	s_{Fe}	$\tilde{J}_{NiNi} \mathbf{0}$ (meV)	$\tilde{J}_{FeFe} \mathbf{0}$ (meV)	$\tilde{J}_{NiFe} \mathbf{0}$ (meV)	$\tilde{J}_{NiNi} \mathbf{k}_X$ (meV)	$\tilde{J}_{FeFe} \mathbf{k}_X$ (meV)	$\tilde{J}_{NiFe} \mathbf{k}_X$ (meV)
1/2	1/2	-215.9	274.6	-517.6	72.0	-91.5	172.5
1/2	1	-215.9	103.0	-316.9	72.0	-34.3	105.6
1/2	3/2	-215.9	54.9	-231.5	72.0	-18.3	77.2

Considering the approximate ratio

$$\tilde{J}_{\beta\beta'} \mathbf{0} \approx 12 J_{\beta\beta'} r_1 \quad (1.3)$$

that is faithfully exclusively for ‘short-range’ magnetic interactions between the 1st nearest neighbors, it is possible to evaluate ‘exchange’ ‘integrals’ for magnetic interactions at the 1st coordination shell radius, r_1 . These results together with the literature data are listed in Table S1.2.

TABLE S1.2. ‘Exchange’ ‘integrals’ for magnetic interactions within the 1st coordination shell, $J_{\beta\beta'} r_1$, for f.c.c.-Ni_{1-c}Fe_c alloys (reported in [4]).

c	s_{Ni}	s_{Fe}	$J_{NiNi} r_1$ (meV)	$J_{FeFe} r_1$ (meV)	$J_{NiFe} r_1$ (meV)	References
$c \in [0, 1]$	1/2	1/2	-17.99	22.88	-43.13	
$c \in [0, 1]$	1/2	1	-17.99	8.58	-26.41	[4]
$c \in [0, 1]$	1/2	3/2	-17.99	4.58	-19.29	
$c \approx 0.75$	1/2	1/2	-22.00	5.00	-22.00	Ni–Fe ^a
$c \approx 0.50$	1/2	1/2	-22.00	5.00	-42.00	Ni–Fe ^a
$c \approx 0.25$	1/2	1/2	-22.00	5.00	-45.00	Ni–Fe ^a
$c \in [0, 1]$	0.3	3/2	-52.00	9.00	-39.00	Ni–Fe ^b
$c \approx 0.50$	0.3	3/2	-30.00	4.00	-30.00	Ni–Fe ^c
$c \approx 0.20$	0.3	3/2	-58.50	23.30	-25.5	Ni–Fe ^c
$c \in [0, 1]$	0.3	1.4	-34.90	1.70	-24.10	Ni–Fe ^d
$c \in [0, 1]$	0.3	1.4	-60.30	2.20	-30.60	Ni–Fe ^e
$c \in [0, 0.5]$	0.3	1.4	-5.30	3.30	-11.40	Ni–Fe ^f
$c \in [0, 0.5]$	0.3	1.4	-16.00	10.10	-35.00	Ni–Fe ^g

^a[7] (cluster variation method), ^b[8] (neutron small-angle scattering technique), ^c[9] (spin-wave resonance method), ^d[10] (cluster methods in the mean-field theory), ^e[11] (Ising-type approximation in Monte Carlo simulation), ^f[12] (mean-field theory vector model and Monte Carlo simulation), ^g[13] (mean-field theory vector model and Monte Carlo simulation).

In Table S1.2, a contradiction in signs of ‘exchange’ ‘integrals’ estimated here and in works of other authors is due to the opposite of $J_{\alpha\alpha'} r_1$ signs in their classical spin Hamiltonians; see original papers in [7–13].

2. ‘Strain-induced’ interatomic-interaction energies of dissolved atoms in solid solutions based on the f.c.c. host metal: the salient features of α -Ni–Fe solutions

The components of the dynamic matrix, $\tilde{\mathbf{A}}(\mathbf{k})$, of a host crystal are as follow [14–16]:

$$\begin{aligned} \tilde{A}_{\mathbf{k}}^{xx} &\approx \frac{1}{4} M \omega_L^2 \left[2 - \cos\left(\frac{a_0 k_x}{2}\right) \cos\left(\frac{a_0 k_y}{2}\right) - \cos\left(\frac{a_0 k_x}{2}\right) \cos\left(\frac{a_0 k_z}{2}\right) \right] + \\ &+ \frac{1}{4} M 2\omega_T^2 - \omega_L^2 \left[1 - \cos\left(\frac{a_0 k_y}{2}\right) \cos\left(\frac{a_0 k_z}{2}\right) \right] + \\ &+ \frac{1}{8} 4a_0 C_{11} - M \omega_L^2 \left[1 - \cos a_0 k_x \right] + \\ &+ \frac{1}{8} 4a_0 C_{44} - M \omega_T^2 \left[1 - \cos a_0 k_y - \cos a_0 k_z \right] \\ \tilde{A}_{\mathbf{k}}^{xy} &\approx a_0 \left(C_{12} + C_{44} \sin\left(\frac{a_0 k_x}{2}\right) \sin\left(\frac{a_0 k_y}{2}\right) \right). \end{aligned} \quad (2.1)$$

In equation (2.1), $\omega_L(\mathbf{k}_X)$ and $\omega_T(\mathbf{k}_X)$ are the longitudinal and transversal frequencies of natural quasi-harmonic vibrations of a host crystal in $X(001)$ -point, M is the host-crystal atom mass (Ni).

When the ‘fictive’ Kanzaki forces in a direct space, $\mathbf{F} \cdot \mathbf{R} - \mathbf{R}'$, are nonzero for the 1st nearest-neighbor coordination shell of sites around the dissolved substitutional atom (β) and are directed along a straight line from the impurity atom towards the host-crystal atom, $\tilde{\mathbf{F}} \cdot \mathbf{k}$ has a following form [16]:

$$\tilde{\mathbf{F}} \cdot \mathbf{k} \cong -i \frac{a_0^2}{4} C_{11} + 2C_{12} L^\beta \begin{vmatrix} \sin\left(\frac{a_0}{2}k_x\right) \left[\cos\left(\frac{a_0}{2}k_y\right) + \cos\left(\frac{a_0}{2}k_z\right) \right] \\ \sin\left(\frac{a_0}{2}k_y\right) \left[\cos\left(\frac{a_0}{2}k_z\right) + \cos\left(\frac{a_0}{2}k_x\right) \right] \\ \sin\left(\frac{a_0}{2}k_z\right) \left[\cos\left(\frac{a_0}{2}k_x\right) + \cos\left(\frac{a_0}{2}k_y\right) \right] \end{vmatrix}. \quad (2.2)$$

TABLE S2.1. The ‘strain-induced’ interaction energies between the substitutional dissolved atoms, $V_{si}^{\beta\beta}(\mathbf{R} - \mathbf{R}')$ ($\beta = \text{Fe}$), in f.c.c. α -Ni host crystal, reported in [15, 17].

$2(\mathbf{R} - \mathbf{R}')/a_0$	110	200	211	220	310	222	321	400	330	411
No. shells	I	II	III	IV	V	VI	VII	VIII	IX _l	IX _u
$ \mathbf{R} - \mathbf{R}' /a_0$	≈ 0.71	1	≈ 1.22	≈ 1.41	≈ 1.58	≈ 1.73	≈ 1.87	2	≈ 2.12	≈ 2.12
$V_{si}^{\text{FeFe}}(\mathbf{R} - \mathbf{R}')$ (meV) ^a	-4.8	-1.3	+0.3	+0.7	-0.3	+0.06	+0.08	-0.2	+0.2	-0.1
$V_{si}^{\text{FeFe}}(\mathbf{R} - \mathbf{R}')$ (meV) ^b	-5.3	-1.5	+0.3	+0.7	-0.4	+0.08	+0.08	-0.2	+0.2	-0.2

^a[15], ^b[17].

TABLE S2.2. Experimental data [18, 19] used in a given work for calculation of ‘strain-induced’ interaction parameters in f.c.c. α -Ni-based solid solutions.

Host crystal	Concentrations of dissolved atoms, c_a	C_{11}, C_{12}, C_{44} (GPa)	$\omega_L \mathbf{k}_X$ (Trad·s ⁻¹)	$\omega_T \mathbf{k}_X$ (Trad·s ⁻¹)	L^{Fe}
α (f.c.c.)-Ni	$c_{\text{Fe}} \in [0, 0.6]$	240, 149, 116 ^a	53.72 ^a	39.40 ^a	+0.033 ^b

^a[18], ^b[19]. Data are given for f.c.c. α -Ni at 300 K.

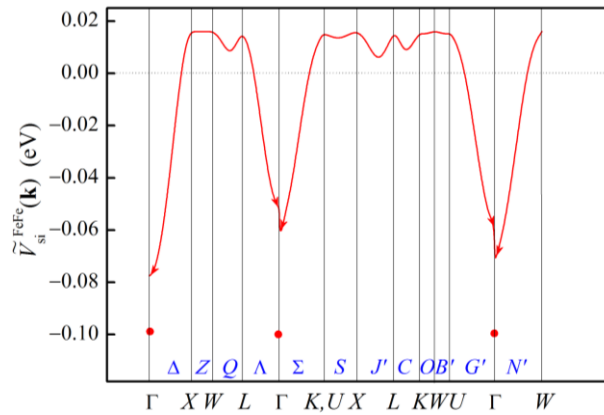


Figure S2.1 Dispersion dependences of ‘strain-induced’ interaction energy Fourier components for dissolved Fe atoms, $\tilde{V}_{si}^{\text{FeFe}}(\mathbf{k})$, in f.c.c. α -Ni along the main directions between the high-symmetry (h-s) points within the irreducible region of the 1st BZ (Fig. 1(b)) at $T = 300$ K. ● is the $\tilde{V}_{si}^{\text{FeFe}}(\mathbf{k}_\Gamma)$. (Compare with Fig. 2 and (14). See [4].)

To calculate the temperature dependences of $\tilde{V}_{si}^{\text{FeFe}}(\mathbf{k}_{\Gamma,h-s}, T)$ for dissolved Fe atoms in f.c.c. α -Ni, we use the approximate semi-phenomenological expressions for quasi-harmonic frequencies of longitudinal and transversal vibrations of a host crystal by means of its lattice parameter and elastic modulus [20]

$$\omega_L(T) \cong \sqrt{\frac{8a_0(T)C_{44}(T)}{M}}, \quad \omega_T(T) \cong \frac{\omega_L(T)}{\sqrt{2}}. \quad (2.3)$$

Here, M is the Ni-atom mass ($9.748 \cdot 10^{-26}$ kg); $C_{44}(T)$, $a_0(T)$ are the temperature-dependent elastic modulus and lattice parameter of a pure f.c.c. Ni, respectively. According to [19], we can represent of $C_{IJ}(T)$ and $a_0(T)$ dependences as $C_{IJ}(T) \approx C_{IJ}(0) + [dC_{IJ}/dT]T$ and $a_0(T) \approx a_0(0) + [da_0/dT]T$. Thus, we obtain: $C_{11,12,44}(0) \approx 264.73$, 151.23, and 133.58 GPa, $dC_{11,12,44}/dT \approx -0.0526$, -0.0052 , and -0.0358 GPa·K $^{-1}$, $a_0(0) \approx 3.4982(7)$ Å, $da_0/dT \approx 6.0 \cdot 10^{-5}$ Å·K $^{-1}$. Substituting the temperature-dependent quantities of $C_{44}(T)$ and $a_0(T)$ into (2.3) and using the approximation of $\omega_{L(T)} \approx \omega_{L(T)}(0) + [d\omega_{L(T)}/dT]T$, we have estimated: $\omega_{L(T)}(0) \approx 61.992$ (43.835) Trad·s $^{-1}$, $d\omega_{L(T)}/dT \approx -0.0083$ (-0.0059) Trad·s $^{-1}$ ·K $^{-1}$. And now, using these data for Fe atoms dissolved in f.c.c. α -Ni host crystal, it is possible to plot the functions of $\tilde{V}_{si}^{\text{FeFe}}(\mathbf{k}_{\Gamma,h-s}, T)$ (Fig. S2.2).

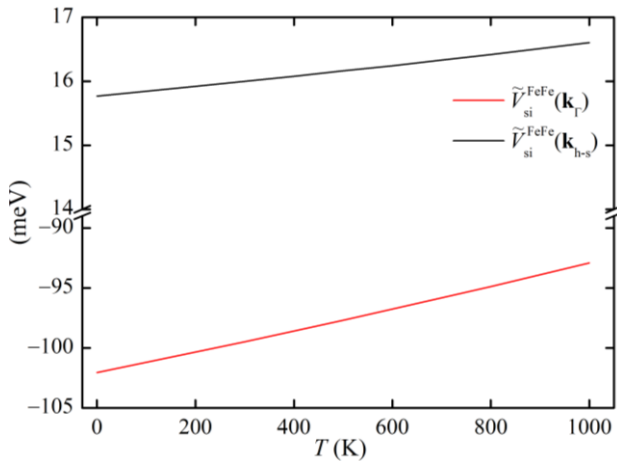


Figure S2.2 Temperature-dependent ‘strain-induced’ interaction energy Fourier components for dissolved Fe-atoms in f.c.c. α -Ni, $\tilde{V}_{si}^{\text{FeFe}}(\mathbf{k})$, calculated for h-s points in the 1st BZ (Fig. 1(b)). It is visible that functions of $\tilde{V}_{si}^{\text{FeFe}}(\mathbf{k}_{\Gamma,h-s}, T)$, linearly depend on temperature and this dependence is very insignificant within the temperature interval 0–1000 K. Therefore, in our calculations we did not take into account the T -dependence of $\tilde{V}_{si}^{\text{FeFe}}(\mathbf{k}, T)$. (See also [4].)

3. ‘Paramagnetic’ ‘mixing’ energy in f.c.c. Ni–Fe alloys

In [4] we have calculated the ‘paramagnetic’ ‘mixing’ energies Fourier components in f.c.c. Ni–Fe alloys as a function of composition, c , and annealing temperatures, T_a . The calculation has been done with use of the KCM formula (1) and experimental data on the diffuse scattering of radiations (both anomalous X-rays and thermal neutrons diffractions) reported over years in [21–32]. The results are illustrated in Fig. S3.1.

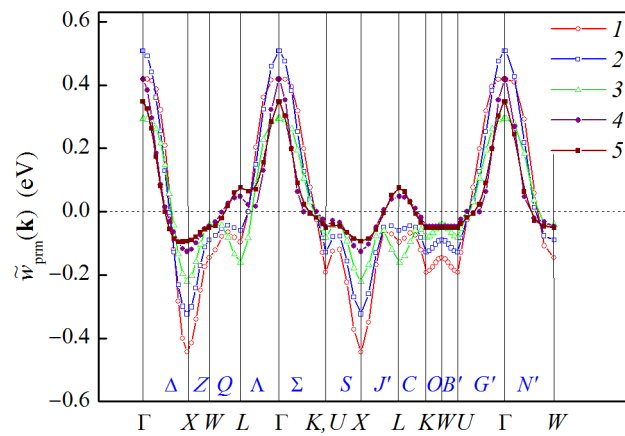


Figure S3.1 Fourier components of ‘paramagnetic’ ‘mixing’ energies, $\tilde{w}_{pm}(\mathbf{k})$, for the h-s points and main symmetry directions within the irreducible region of the 1st BZ (Fig. 1(b)) for f.c.c. Ni–Fe alloys at different isothermal-annealing temperatures, T_a , and concentrations of Fe atoms, c_{Fe} . 1— $\text{Ni}_{0.775}\text{Fe}_{0.225}$ at $T_a = 1273$ K, 2— $^{62}\text{Ni}_{0.765}\text{Fe}_{0.235}$ at $T_a = 808$ K, 3— $\text{Ni}_{0.535}\text{Fe}_{0.465}$ at $T_a = 1273$ K, 4— $\text{Fe}_{0.632}\text{Ni}_{0.368}$ at $T_a = 753$ K, 5— $\text{Fe}_{0.698}\text{Ni}_{0.302}$ at $T_a = 743$ K. For presented calculations, we used the experimental diffuse scattering data reported in [21–32].

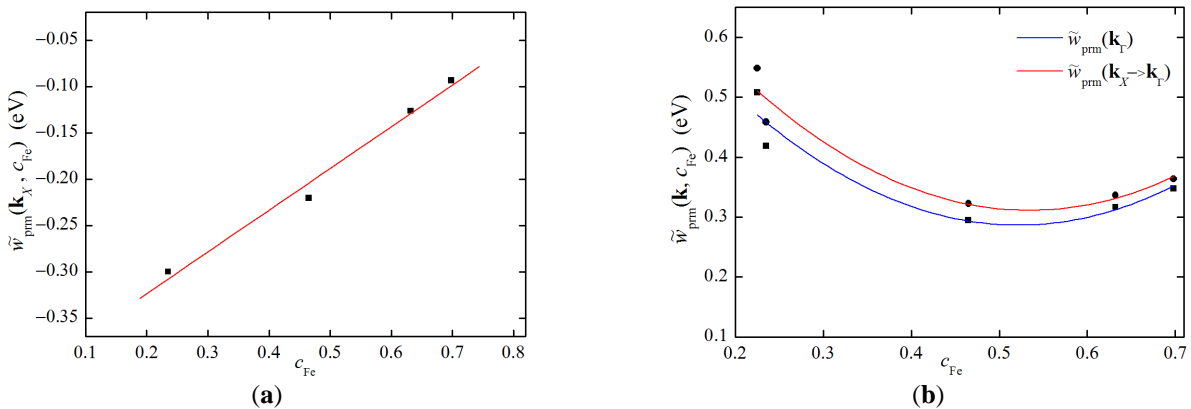


Figure S3.2 Concentration dependences of the ‘paramagnetic’ ‘mixing’ energies Fourier components, $\tilde{w}_{\text{prm}}(\mathbf{k}, c_{\text{Fe}})$, for some quasi-wave-vectors within the 1st BZ, $\mathbf{k} = \mathbf{k}_X$ (a), $\mathbf{k} = \mathbf{k}_{\Gamma} = \mathbf{0}$ and $\mathbf{k}_{\downarrow \mathbf{k}_X} \rightarrow \mathbf{0}$ (b), for f.c.c. Ni–Fe alloys. ■—data extracted from Fig. S3.1 (here the ‘mixing’-energies were calculated on the basis of diffuse scattering experiments reported in [21–32]), ●—data calculated in [4]. Lines—polynomials presented in Table S3.1.

TABLE S3.1. Coefficients of concentration dependences of the ‘paramagnetic’ ‘mixing’ energy Fourier components, $\tilde{w}_{\text{prm}}(\mathbf{k}, c)$, approximately described by the 1st- or 2nd-degree polynomials, $K_0(\mathbf{k}) + K_1(\mathbf{k})c$ or $K_0(\mathbf{k}) + K_1(\mathbf{k})c + K_2(\mathbf{k})c^2$ (Figs. S3.2 (a) and (b)), for f.c.c. Ni–Fe alloys, obtained by fitting the estimated diffuse scattering data taken from Fig. S3.1 (see [4]).

Quasi-wave-vectors	$K_0(\mathbf{k})$ (eV)	$K_1(\mathbf{k})$ (eV)	$K_2(\mathbf{k})$ (eV)	Mean-square deviation, R^2	Fitting	Comments
$X(0\ 0\ 1)$	−0.414	0.450	—	0.986	1 st degree	Extracted from
$X(0\ 0\ 1) \rightarrow \Gamma(0\ 0\ 0)$	0.855	−2.177	2.087	0.900	2 nd degree	single-crystal data
$\Gamma(0\ 0\ 0)$	0.843	−2.339	2.344	0.916	2 nd degree	[21–32]

References

- [1] Tatarenko, V. A. & Radchenko, T. M. (2003). *Intermetallics*, **11**, 1319–1326.
- [2] Bokoch, S. M. & Tatarenko, V. A. (2008). *Solid State Phenomena*, **138**, 303–318.
- [3] Tatarenko, V. A., Bokoch, S. M., Nadutov, V. M., Radchenko, T. M. & Park, Y. B. (2008). *Defect and Diffusion Forum*, **280–281**, 29–78.
- [4] Bokoch, S. M. & Tatarenko, V. A. (2010). *Uspehi Fiziki Metallov*, **11**, 413–460.
- [5] Swartzendruber, L. J., Itkin, V. P. & Alcock, C. B. (1991). *J. Phase Equil.* **12**, 288–312.
- [6] Men’shikov, A. Z. & Yurchikov, E. E. (1972). *Izv. Akad. Nauk SSSR. Ser. Fiz.* **36**, 1463–1467.
- [7] Lawrence, P. J. & Rossiter, P. L. (1986). *J. Phys. F: Met. Phys.* **16**, 543–556.
- [8] Hatherly, M., Hirakawa, K., Lowde, R. D., Mallett, J. F., Stringfellow, M. W. & Torrie, B. H. (1964). *Proc. Phys. Soc.* **84**, 55–62.
- [9] Maeda, T., Yamauchi, H. & Watanabe, H. (1973). *J. Phys. Soc. Japan*, **35**, 1635–1642.
- [10] Dubé, M., Heron, P. R. L. & Rancourt, D. G. (1995). *J. Magn. Magn. Mater.* **147**, 122–132.
- [11] Dang, M.-Z., Dubé, M. & Rancourt, D. G. (1995). *J. Magn. Magn. Mater.* **147**, 133–140.
- [12] Taylor M. B. & Gyorffy, B. L. (1992). *J. Magn. Magn. Mater.* **104–107**, 877–878.
- [13] Taylor, M. B., Gyorffy, B. L. & Walden, C. J. (1991). *J. Phys. Condens. Matter*, **3**, 1575–1587.
- [14] Kushwaha, M. S. & Kushwaha, S. S. (1978). *Phys. Status Solidi B*, **87**, 247–253.
- [15] Tatarenko, V. A. & Nadutov, V. M. (2004). *Uspehi Fiziki Metallov*, **5**, 503–534.
- [16] Bugaev, V. N. & Tatarenko, V. A. (1989). *Interaction and Arrangement of Atoms in Interstitial Solid Solutions Based on Closed-Packed Metals*. Kiev: Naukova Dumka.
- [17] Beiden, S. V. & Vaks, V. G. (1992). *Physics Letters A*, **163**, 209–213.
- [18] Birgeneau, R. J., Cordes, J., Dolling, G. & Woods, A. D. B. (1964). *Phys. Rev. A*, **136**, 1359–1365.
- [19] Pearson, W. B. (1958). *Handbook of Lattice Spacing and Structure of Metals and Alloys*. Vol. 1. New York: Pergamon Press; Pearson, W. B. (1968). *Handbook of Lattice Spacing and Structure of Metals and Alloys*. Vol. 2. New York: Pergamon Press; Pearson.
- [20] Tatarenko, V. A. & Tsinman, K. L. (1992). *Metallofizika*, **14**, 14–36.

- [21] Lefebvre, S., Bley, F., Bessière, M., Fayard, M., Roth, M. & Cohen, J. B. (1980). *Acta Cryst. A* **36**, 1–7.
- [22] Lefebvre, S., Bley, F., Fayard, M., & Roth, M. (1981). *Acta Metall.* **29**, 749–761.
- [23] Bley, F., Amilius, Z. & Lefebvre, S. (1988). *Acta Metall.* **36**, 1643–1652.
- [24] Ice, G. E., Sparks, C. J., Habenschuss, A. & Shaffer, L. B. (1992). *Phys. Rev. Lett.* **68**, 863–866.
- [25] Jiang, X., Ice, G. E., Sparks, C. J. & Zschack, P. (1995). *Mat. Res. Soc. Symp. Proc.* **375**, 267–273.
- [26] Jiang, X., Ice, G. E., Sparks, C. J., Robertson, L. & Zschack, P. (1996). *Phys. Rev. B*, **54**, 3211–3226.
- [27] Ice, G. E., Sparks, C. J., Robertson, J. L., Epperson, J. E. & Jiang, X. (1996). *Mat. Res. Soc. Symp. Proc.* **437**, 181–186.
- [28] Ice, G. E., Painter, G. S., Shaffer, L., Sparks, C. J., Averill, F. W. & Jiang, X. (1996). *NanoStructured Materials*, **7**, 147–160.
- [29] Ice, G. E., Sparks, C. J., Jiang, X. & Robertson, J. L. (1998). *J. Phase Equil.* **19**, 529–537.
- [30] Ice, G. E. & Sparks, C. J. (1999). *Annu. Rev. Mater. Sci.* **29**, 25–52.
- [31] Robertson, J. L., Ice, G. E., Sparks, C. J., Jiang, X., Zschack, P., Bley, F., Lefebvre, S. & Bessiere, M. (1999). *Phys. Rev. Lett.* **82**, 2911–2914.
- [32] Cenedese, P., Bley, F. & Lefebvre, S. (1984). *Mat. Res. Soc. Symp. Proc.* **21**, 351–353.